



Enhancing the Curing Efficiency and Physicochemical Properties of Acrylated Epoxidized Palm Oil Polyurethane Coatings via Double Acrylation-Thiol Modification

Siti Noor Hidayah Mustapha¹ · Mohamad Ismail Mohamad Isa¹ · Muhammad Safwan Shamsuddin¹ · Rasidi Roslan¹ · Rohani Mustapha² · Mohd Jumain Jalil³

Accepted: 3 May 2025 / Published online: 29 May 2025

© The Author(s) 2025

Abstract

The slow curing and suboptimal properties of epoxidized palm oil polyurethane acrylate (EPOUA) coatings remain significant challenges that limit their performance. This study enhances these coatings by applying acrylation-thiol (AT) modification onto the EPOUA coatings provided double acrylation-thiol effect to the EPOUA. EPOUA and AT were first synthesized separately, then the AT was blended at concentrations of 2, 4, 6, and 8 parts per hundred resin (phr) EPOUA. The blended mixture was then cast onto a silicone mold with a thickness of 1 mm and cured using ultraviolet (UV) radiation. The results show that 2 and 4 phr AT significantly improved curing, reducing time by 15 and 30 s, respectively. Crosslinking density also increased, with gel content rising by 6% and 9% at 2 and 4 phr AT, respectively, while maintaining low volatile organic compound (VOC) emissions (<5%). Physical properties improved, with hardness increasing threefold at 2 phr AT and fourfold at 4 phr AT on glass, plywood, and steel. Adhesion remained excellent (5B rating) on plywood, steel, and aluminum. However, higher AT concentrations (6 and 8 phr) resulted in inconsistent curing and increased VOC emissions. These findings indicate that 4 phr AT optimally improves EPOUA coatings' curing efficiency, crosslinking, and mechanical properties while maintaining environmental compliance.

Keywords UV-curing · Palm oil · Biocoating · Thiolation · Acrylation · Physicochemical

Introduction

The demand for environmentally friendly coatings has driven the shift toward using renewable resources as raw materials for UV-curable coatings. Vegetable oils (VOs) have been widely explored due to their abundant availability and chemical versatility, possessing functional groups such as

double bonds, epoxies, hydroxyls, and esters, which enable various chemical modifications (Rahman et al. [22]). Typically, drying and semi-drying VOs are preferred in surface coatings since they undergo natural oxidative crosslinking, enhancing film formation (Abu Bakar et al. [1]). However, palm oil, classified as a non-drying oil due to its low unsaturation content, has limited direct applicability in coatings without structural modification (Ooi et al. [19]). Despite its extensive use in food and cosmetics, palm oil has recently gained attention in composite and coating applications, such as a diluent in diamond-like carbon coatings (Kadir et al. [12]), a healing agent in petroleum-based coatings, and a flexibility enhancer in polyaniline-based conductive coatings (Hashim et al. [ahmood et al., 8]). Additionally, palm oil waste has been explored as a filler for concrete coatings (Ali et al. [2]). However, the direct use of palm oil as the main component in bio-based coatings remains limited due to its low functionality and non-drying nature, necessitating further chemical modifications to improve its performance.

✉ Siti Noor Hidayah Mustapha
snhidayah@ump.edu.my

¹ Faculty of Industrial Sciences and Technology, Universiti Malaysia Pahang Al-Sultan Abdullah, Lebuhr Persiaran Tun Khalil Yaakob, Kuantan, Pahang 26300, Malaysia

² Faculty of Ocean Engineering Technology and Informatics, Universiti Malaysia Terengganu, Kuala Nerus 21030, Terengganu, Malaysia

³ Chemical Engineering Studies, College of Engineering, Universiti Teknologi MARA (UiTM) Cawangan Johor, Kampus Pasir Gudang, Masai 81750, Johor, Malaysia

To enhance the curing efficiency and physicochemical properties of palm oil-based polyurethane coatings, chemical modifications such as acrylation have been widely studied. One of the most common approaches involves introducing acrylate groups to form epoxidized palm oil polyurethane acrylate (EPOUA), which can then be combined with a photoinitiator to enable UV curing through free radical polymerization (Kosheela et al. [14]). This method has been applied in bio-coatings, inks, and adhesives (Cheong et al. [5]). However, previous studies indicate that acrylated palm oil bio-coatings exhibit poor UV curing and mechanical performance, including low hardness and adhesion, compared to synthetic coatings (Teo et al. [26]; Salih et al. [23]; Tajau et al. [25]). For instance, Tajau et al. [25] reported that modified palm oil (urethane acrylate and acrylate epoxy) bio-coatings for wood applications exhibited 10–15% lower performance and crosslinking density than synthetic coatings. The degree of crosslinking, influenced by the modification method, significantly affects the curing rate and energy requirements.

The UV-curing process involves free radical polymerization, where photoinitiator-generated free radicals trigger rapid chain-growth reactions. This allows UV-curable coatings to cure within seconds, making them more efficient than conventional coatings, which may require hours or days to fully cure (Smith et al. [24]). In addition, UV-curable coatings provide superior mechanical properties, such as increased hardness and scratch resistance. Despite these benefits, oxygen inhibition remains a major limitation, leading to incomplete curing and surface tackiness. Oxygen interferes with polymerization by scavenging free radicals, reducing overall crosslinking efficiency (Ligon et al. [15]). To address this issue, researchers have developed formulations with enhanced acrylate functionality, increased double-bond concentration, and the addition of reactive components such as ethers, amines, and thiols (Bowman and Kloxin [4]). Recent studies highlight that thiol-ene reactions, where thiols react with carbon-carbon double bonds, significantly enhance curing efficiency under mild conditions, making them a promising strategy for overcoming oxygen inhibition (Hoyle and Bowman [10]).

Despite these advances, the existing modifications of palm oil-based polyurethane coatings still suffer from suboptimal curing performance, mechanical properties, and environmental concerns. While acrylation improves functionality, it does not fully resolve the oxygen inhibition issue, leading to incomplete polymerization and reduced crosslinking density. Additionally, previous studies have not adequately explored the balance between curing efficiency, mechanical strength, and environmental sustainability. There is a lack of research on optimizing double acrylation-thiol modification as a strategy to overcome these limitations, particularly

in achieving improved adhesion, hardness, and crosslinking density while maintaining eco-friendliness. Therefore, this study focuses on enhancing the curing efficiency and physicochemical properties of epoxidized palm oil polyurethane acrylate (EPOUA) coatings through double acrylation-thiol modification. This novel approach aims to mitigate oxygen inhibition while improving crosslinking density, adhesion, and hardness. The research evaluates curing behavior using ATR-FTIR, DSC, and XRD, while crosslinking density is assessed through gel content and VOC release analysis. Furthermore, the physical properties, including hardness and adhesion, are analyzed using pencil scratch tests and adhesion tests on various substrates such as glass, plywood, steel, and aluminum to determine the optimal application of the modified coating.

Methodology

Materials

The main material used was epoxidized palm oil (EPO), which was obtained from PolyGreen (M) Sdn. Bhd. (specifications: oxirane oxygen content, OOC = 2.7–2.9%, $M_w = 848.75$ Da, moisture content = 0.3%). Acrylic acid (99% concentration), triethylamine (TEA), hydroxyethyl acrylate (HEA), isophorone diisocyanate (IPDI), dibutyltin dilaurate (DBTDL), hydroquinone, 1,2-ethanedithiol (> 98.0% gas chromatography grade solvent), sodium sulfite, and formaldehyde 37%, stabilized in methanol, and 37% acid hydrochloric (HCl) stabilized in water were purchased from Aldrich Chemical Co. Inc., USA. Trimethylpropane triacrylate (TMPTA) and 1,6-hexanediol diacrylate (HDDA) were acquired from UCB Chemicals Sdn. Bhd., Malaysia. Benzophenone, which was used as a photoinitiator, was purchased from Ciba Specialty Chemicals Inc., Switzerland. Sodium metabisulfite was purchased from Baker (metabisulfite converts to bisulfite in an aqueous solution). All chemicals were used as received without further purification.

Methodology

Preparation of Acrylation Thiol (AT) Mixture

A total of 0.0033 mol of 1,2-ethanedithiol and 0.0033 mol of TMPTA were mixed in a glass beaker with magnetic stirring at ambient temperature until fully combined. Subsequently, 0.2 mol of formaldehyde, 0.1 mol of bisulfite, and 0.01 mol of sulfite were added and mixed until a homogeneous solution was achieved, for up to 5 min. Next, 2 ml of HCl was added to terminate the reaction, and the mixture was immediately filtered. The filtrate was then dried at 80 °C until

constant weight was obtained. This method was adopted from Hu et al. [11]).

Preparation of Epoxidized Palm Oil Polyurethane Acrylate (EPOUA) Oligomer

The synthesis of EPOUA began with the preparation of acrylated epoxidized palm oil (AEPO). A three-neck round-bottom flask equipped with a condenser, dropping funnel, and thermometer was prepared. EPO was added and mixed with 1% (w/w) hydroquinone and 1% (w/w) TEA. Then, acrylic acid at a 1:4 molar ratio to EPO was added dropwise. The mixture was stirred for approximately 15 h at a constant temperature of 110 °C. Subsequently, the mixture was quenched with petroleum ether overnight and further washed with distilled water. AEPO was dried using a rotary evaporator at 90 °C until a constant weight was obtained, following the methodology published in our previous work (Mohamad Isa and Mustapha [16]; Mohamad Isa et al. [17]).

Then, 1 mol of HEA, 1 mol of IPDI, 0.05% (w/w) hydroquinone, and 1% (w/w) DBTL were added to the AEPO and stirred until fully miscible for 15 min to form the epoxidized palm oil polyurethane acrylate (EPOUA) oligomer.

Preparation of EPOUA-AT Film

The unmodified EPOUA film was used as the control system which consist of 60/20/20 (wt%) of EPOUA/HDDA/TMPTA. In AT modified system, the 60 g of EPOUA oligomer was firstly mixed with the varying concentrations of AT (2 g, 4 g, 6 g, and 8 g, corresponding to 2, 4, 6, and 8 parts per hundred resin (phr)). The mixture was stirred at 50 °C for 18 h to form the EPOUA-AT oligomer. Subsequently, the remaining resin components which are: 20 g TMPTA, 20 g HDDA, and 4% (w/w) benzophenone were added and stirred continuously until fully miscible. The final solution was cast onto 10 cm × 10 cm glass plate at a 1 mm thickness, controlled using a film applicator. The coated samples were then cured under UV radiation (1200 W) at varying exposure times, up to 105 s at 15 s interval until fully cured. The sample casting was repeated on plywood and steel substrate to further analysed their physical properties.

Characterization

The preparation process of AT, EPOUA and EPOUA-AT was characterized using Fourier Transform Infrared Spectroscopy (FTIR) Model Prestige-21, Shimadzu, Japan in the attenuated total reflection (ATR) mode. The liquid mixture was directly poured onto the ATR crystal and the sample was scanned from 700 cm⁻¹ to 4000 cm⁻¹ to obtained the result.

For the curing speed analysis, the sample was exposed to UV radiation for up to 105 s. At every 15-second intervals, the sample was analyzed to determine its curing behavior using ATR-FTIR, differential scanning calorimetry (DSC), and X-ray diffraction (XRD). The DSC test was conducted by heating the sample from 30 °C to 300 °C at a constant heating rate of 10 °C/min. The energy profile is evaluated to analyse its curing behaviour. In the XRD test, the sample was first dried before analysis and directly analyzed without any additional preparation. Cu-K α radiation was used as the radiation source, with a scanning range of 5–80° at a scan rate of 5°/min.

Further analysis of the effect of AT on the crosslinking density and physical properties of EPOUA was conducted using the gel content (Gc) test (ASTM D2765-01) and the volatile organic compound (VOC) test (ASTM D2369). For this analysis, fully cured samples (maintained at 90 s of UV curing) were selected.

For the Gc test, a 1 g sample was dried at 40 °C for two days before testing. The dried sample was placed in an empty filter paper pouch, and the initial weights of the empty pouch (W1) and the pouch containing the dried film (W2) were recorded. The pouch was then sealed and weighed (W3). Next, the sealed pouch containing the film was immersed in acetone for 24 h, then dried at 150 °C until a constant weight (W4) was obtained. Each sample was analyzed in triplicate to determine the average value. The Gc of the cured films was calculated using Eq. 1.

For the VOC test, the cured samples were weighed before and after being baked at 115 °C for one hour. The percentage of volatile organic compounds was determined using Eq. 2.

$$\text{Gel Content, \%} = 100 - \left(\frac{W_3 - W_4}{W_2 - W_1} \right) \times 100 \quad (1)$$

$$\text{VOC, \%} = \frac{\text{Final weight of sample} - \text{Initial weight of sample}}{\text{Initial weight of sample}} \times 100 \quad (2)$$

Physical analysis was conducted using a pencil hardness test, scanning electron microscopy (SEM), and an adhesion test. In this test, the fully cured sample was chosen as comparison at different concentration of AT modification.

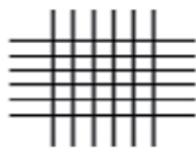
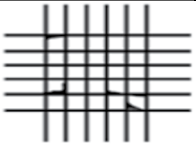
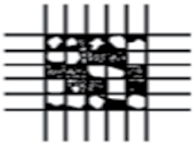
For the hardness analysis, a series of pencils with varying hardness levels (6B–6 H) were dragged along the film surface using a pencil hardness tester (HT6510P) under constant force (2 kg load). The scratch resistance was evaluated according to ASTM D3363. Hardness of the coating was determined by the resistance of a coating to indentation or scratching. Test was conducted from the hardest (6 H) to the softness pencil (6B).

The surface morphology of the sample was analyzed using scanning electron microscopy (SEM). Prior to observation, the sample was coated with a 2 nm thick gold-palladium layer. SEM imaging was performed using a JSM-7200 F microscope at a magnification of 2500 \times with an acceleration voltage of 10 kV.

For the adhesion test, method B of ASTM D3359, which is more suitable for laboratory use, was applied. A lattice

pattern with six cuts in each direction was made through the film down to the substrate. A pressure-sensitive tape was then applied over the lattice pattern and subsequently removed. The adhesion was assessed qualitatively using a 0–5B rating scale, as shown in Table 1.

Table 1 ASTM D3359 classification of adhesion test result

Classification	Percent Area Removed	Surface of Crosscut Area	Description
5B	0% None		The edges of the cuts are completely smooth; none of the squares of the lattice is detached.
4B	Less than 5%		Small flakes of the coating are detached at intersections; less than 5 % of the area is affected.
3B	5–15%		Small flakes of the coating are detached along edges and at intersections of cuts. The area affected is 5 to 15 % of the lattice.
2B	15–35%		The coating has flaked along the edges and on parts of the squares. The area affected is 15 to 35 % of the lattice.
1B	35–65%		The coating has flaked along the edges of cuts in large ribbons and whole squares have detached. The area affected is 35 to 65 % of the lattice.
0B	Greater than 65%		Flaking and detachment worse than classification 1B.

Result and Discussion

Characterization of EPOUA at Different Acrylation-Thiol (AT) Addition

Figure 1 presents the FTIR spectra of EPOUA, AT, and the uncured EPOUA-AT mixture with 2, 4, 6, and 8 phr AT additions. The spectra reveal the disappearance of the S-H functional group peak at 2555.52 cm^{-1} in the AT mixture upon reaction with EPOUA. Additionally, a new peak observed at 711.95 cm^{-1} in the EPOUA-AT spectra corresponds to the formation of the C-S functional group. The broad OH peak at 3423 cm^{-1} , present in the AT mixture, diminished in the EPOUA-AT spectra, indicating that pre-polymerization had occurred during the reaction. This suggests that the thiol-ene click reaction between EPOUA and AT successfully took place. Other characteristic peaks, such as the sharp C=O peak at 1722 cm^{-1} and the C=C peak at 1634 cm^{-1} , remained consistent across all EPOUA-AT mixture compositions, confirming the successful acrylation-thiol (AT) addition to the EPOUA mixture.

Curing Speed Analysis of EPOUA at Different Acrylation-Thiol (AT) Addition and UV Exposure Time

Fourier Transform Infra-red Spectroscopy (FTIR)

Curing analysis was conducted using FTIR spectroscopy. Figure 2 presents the FTIR spectra of EPOUA-AT with 0, 2, 4, 6, and 8 phr AT, cured under UV radiation for varying durations (0, 15, 30, 45, 60, 75, 90, and 105 s). The spectra indicate that increasing UV exposure time results in a reduction of the C=C functional group peaks at approximately

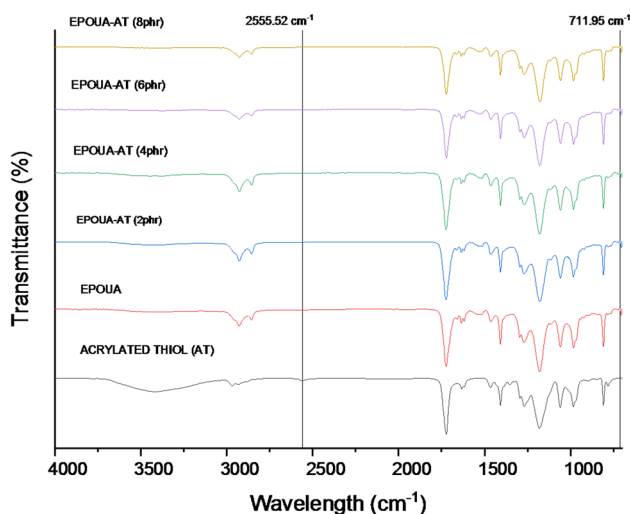


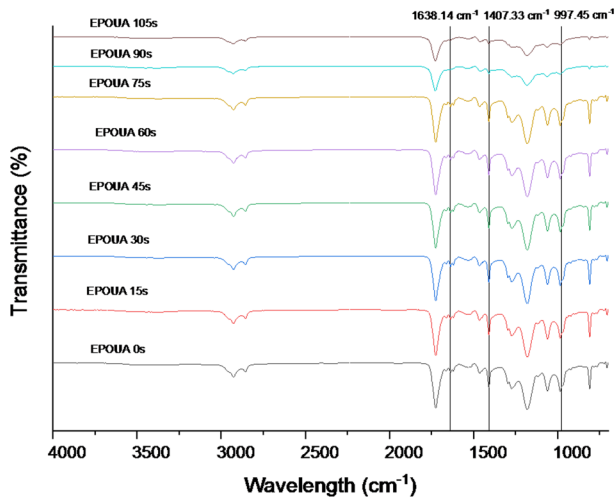
Fig. 1 FTIR analysis of TMPTA-thiol (acrylated thiol - AT), EPOUA, and EPOUA-AT at 2,4,6 and 8 phr

1600 cm^{-1} and 997.45 cm^{-1} , along with the CH functional group peak around 1400 cm^{-1} , signifying successful polymerization and curing. The free radicals generated from benzophenone initially attack the CH bond, propagate to the C=C functional groups, and trigger the crosslinking process. Complete curing was achieved at 90 s for pure EPOUA (0 phr AT), as evidenced by the complete disappearance of the C=C peaks. With the addition of 2 phr AT, the curing time decreased to 75 s, while at 4 phr, it further reduced to 60 s. However, for both 6 and 8 phr additions, the curing time plateaued at 60 s. These results suggest that the optimal addition of 4 phr AT enhanced the curing speed of EPOUA by reducing the required curing time by 30 s.

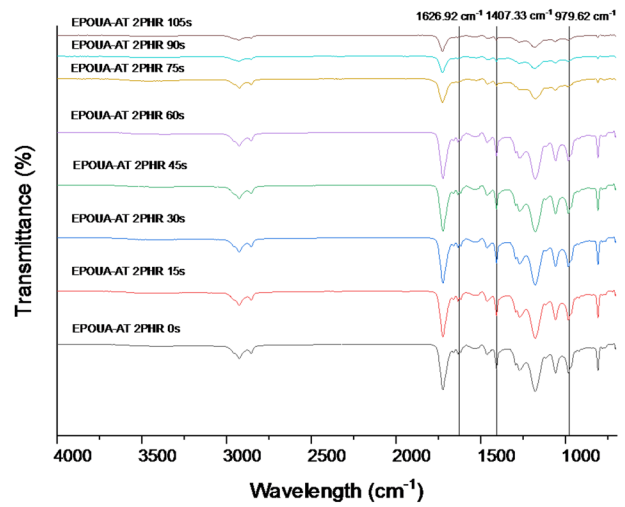
Differential Scanning Calorimetry (DSC)

Figure 3 presents the DSC curves for samples containing 0 to 8 phr AT, measured from 30 to $300\text{ }^{\circ}\text{C}$. The DSC curves reveal the presence of a glass transition temperature (T_g) between 4 and $6\text{ }^{\circ}\text{C}$, crystallization between 90 and $140\text{ }^{\circ}\text{C}$, and curing phases (onset curing temperature) from $210\text{ }^{\circ}\text{C}$ to $275\text{ }^{\circ}\text{C}$, as summarized in Table 2. However, the complete curing peak (T_{cure}) could not be clearly observed, as it occurred above $300\text{ }^{\circ}\text{C}$. The DSC profiles indicate that both EPOUA and EPOUA-AT exhibit semicrystalline behavior. Table 2 shows that all samples had T_g values below $10\text{ }^{\circ}\text{C}$, reflecting the soft segment properties of the material. T_g generally increased with longer UV exposure times across all AT concentrations, likely due to early crosslinking during initial UV exposure, which restricted molecular chain mobility and enhanced intermolecular interactions. This led to improved resistance to thermal strain as the degree of crosslinking increased, aligning with the findings of Parasakar et al. [21], who studied the effect of chemical crosslinking on polyurethane systems.

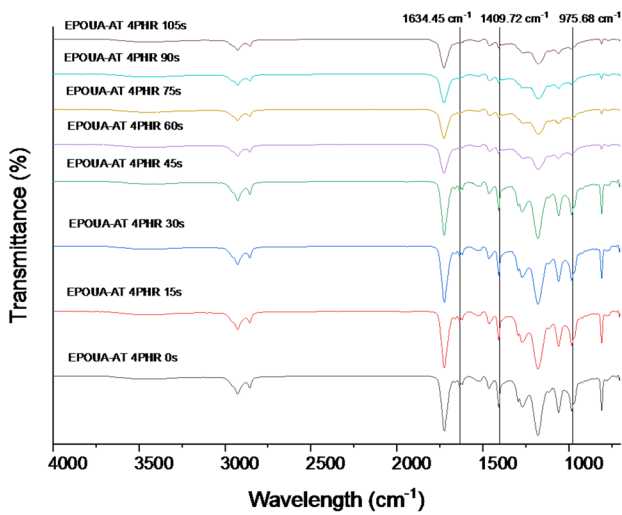
The onset curing temperature (T_{oc}) for pure EPOUA increased from $212\text{ }^{\circ}\text{C}$ at 0 s to $257\text{ }^{\circ}\text{C}$ at 75 s of UV exposure. It then slightly decreased and stabilized at $252\text{ }^{\circ}\text{C}$ at 90 and 105 s, indicating complete curing at 90 s. For a 2 phr AT addition, the curing temperature increased from $225\text{ }^{\circ}\text{C}$ to $258\text{ }^{\circ}\text{C}$ between 0 and 60 s, stabilizing at $255\text{ }^{\circ}\text{C}$ at 75 s, indicating complete curing at 60 s. Similarly, for a 4 phr AT addition, the curing temperature increased from $233\text{ }^{\circ}\text{C}$ to $260\text{ }^{\circ}\text{C}$ (0–60 s) and slightly decreased to $259\text{ }^{\circ}\text{C}$ at 75 s. The 6 and 8 phr AT additions followed a similar trend, with curing temperature decreasing after 75 s. However, inconsistent results were observed with longer UV exposure, likely due to increased structural complexity resulting from higher crosslinking. A higher T_{oc} corresponds to a higher degree of crosslinking. Thus, these findings demonstrate that the addition of 2 and 4 phr AT significantly enhances the curing performance of EPOUA-AT samples.



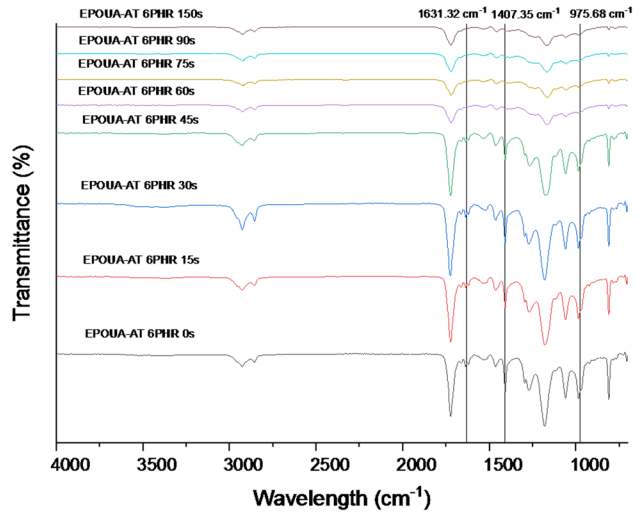
(a)



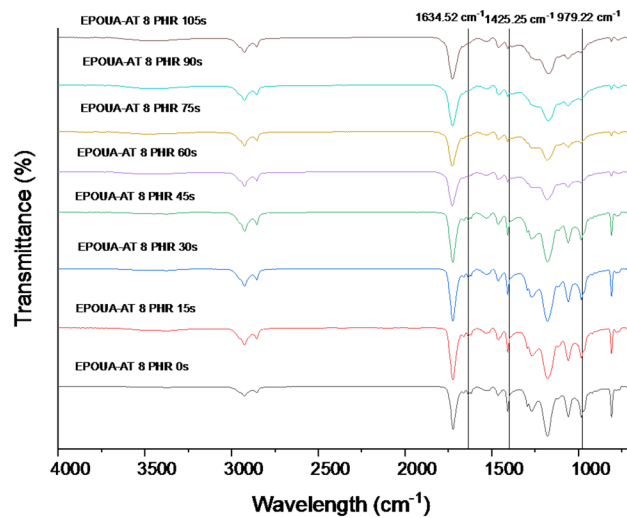
(b)



(c)



(d)



(e)

Fig. 2 FTIR Analysis of EPOUA at Different Acrylation-Thiol (AT) addition and UV Exposure Time: (a) 0phr AT, (b) 2phr AT, (c) 4phr AT, (d) 6phr AT, and (e) 8phr AT

X-ray Diffraction (XRD)

Figure 4 shows the XRD results of EPOUA-AT at different UV curing time. Generally, all XRD patterns exhibited a broad peak around 20° and a sharp peak at 30°, likely corresponding to their semicrystalline nature (Mudri et al. [18]). As the curing period for EPOUA-AT increased (from 0 to 105 s) for all concentrations, the broad peak region showed an increase in intensity, while the crystalline peak at 30° decreased. This trend could be attributed to urethane linkage formation and the crosslinking process occurring between urethane chains during curing (Paraskar and Kulkarni [20]). Based on the results, the sharp crystalline peak observed at 0 s gradually decreased with increasing UV exposure time during curing for all samples with 0, 2, 4, 6, and 8 phr AT additions. This peak diminished in intensity and eventually disappeared after a certain curing period. For 0 phr AT, the peak disappeared at 105 s of curing. At 2 and 4 phr AT, the peak vanished at 90 and 75 s, respectively. For 6 and 8 phr AT, the peak disappeared at 90 s. It can be inferred that the crystalline phase undergoes crosslinking, forming a complex semicrystalline polymeric arrangement (He et al. [9]). In conclusion, the addition of AT improved the curing speed of the EPOUA samples.

Crosslinking Density Analysis of EPOUA and EPOUA-AT at Different Concentrations

Gel Content Test and Volatile Organic Compound (VOC) Test

Table 3 presents the gel content and VOC release of EPOUA at different AT additions. The results indicate that increasing AT additions leads to higher gel content values, signifying an increase in the crosslinking density of the EPOUA samples. The most significant improvement was observed with the addition of 2 phr AT, where the gel content of EPOUA increased by 7.71%, from 74.21 to 80.42%. Further increasing AT from 2 phr to 4 phr resulted in an additional 5.6% improvement, raising the gel content to 85.2%. However, increasing AT from 4 phr to 6 phr and from 6 phr to 8 phr resulted in only slight improvements of 2.1% and 1.6%, respectively. These findings suggest that while AT enhances crosslinking density, excessive AT concentrations may eventually limit crosslinking due to the increased compactness of the polymer molecules, restricting further network formation.

In the other hand, increasing AT additions led to a higher VOC release percentage, reflecting the fact that AT is a simpler molecular compound that can evaporate more easily.

Considering the error margin, the addition of 2 phr AT maintained the VOC release of EPOUA. This phenomenon suggests that 2 phr AT provides optimal bonding within the EPOUA structure, whereas increasing AT concentrations introduce excess unbonded AT molecules, contributing to higher VOC content. According to the U.S. Environmental Protection Agency (EPA) regulations, the VOC limit for industrial maintenance coatings is 450 g/L, while for paints applied to flat surfaces, the limit is 250 g/L (EPA [7]). Due to health and environmental concerns, some manufacturers comply with more stringent standards, setting the VOC limit at 50 g/L for all finishes (Consumer Reports [6]). Based on the results in Table 7, AT additions up to 4 phr are considered acceptable, as the VOC release remains below 5% (50 g/L).

Figure 5 illustrates the relationship between volatile organic compound (VOC) emissions and gel content at varying acrylation-thiol (AT) concentrations in EPOUA. The data indicate that increasing AT levels enhance the crosslinking density of EPOUA-AT, attributed to the additional C=C bonds from AT facilitating more extensive polymerization. Notably, gel content shows significant increases at 2 and 4 parts per hundred resin (phr) AT additions, while 6 and 8 phr additions result in only slight improvements. This trend suggests that higher AT concentrations (6 and 8 phr) lead to a more compact polymer network, which may restrict further crosslinking during polymerization. Concurrently, escalating AT additions correlate with increased VOC emissions, likely due to the low molecular weight of AT, making it more prone to evaporation. Despite the rise in VOC emissions, the increase is gradual at 2 and 4 phr AT additions, whereas 6 and 8 phr additions cause a pronounced surge in VOC release. Therefore, based on Fig. 2, a 4 phr AT addition achieves the optimal balance between maximizing gel content and minimizing VOC emissions.

Physical Properties Analysis of EPOUA and EPOUA-AT at Different Concentrations

Scratch Test

Tables 4, 5 and 6 presents the hardness test results of EPOUA-AT coatings at different concentrations on glass, plywood, and steel substrates. The hardness of these coatings ranged from H to 5 H for glass, H to 4 H for plywood, and 8 H to 4 H for steel. In general, the addition of acrylation thiol (AT) led to a reduction in hardness across all substrates. This decrease is likely due to the increased flexibility introduced by AT, which enhances crosslinking but may reduce the overall rigidity of the polymer network. Despite the observed reduction, the hardness values for all AT concentrations remained within an acceptable range. According

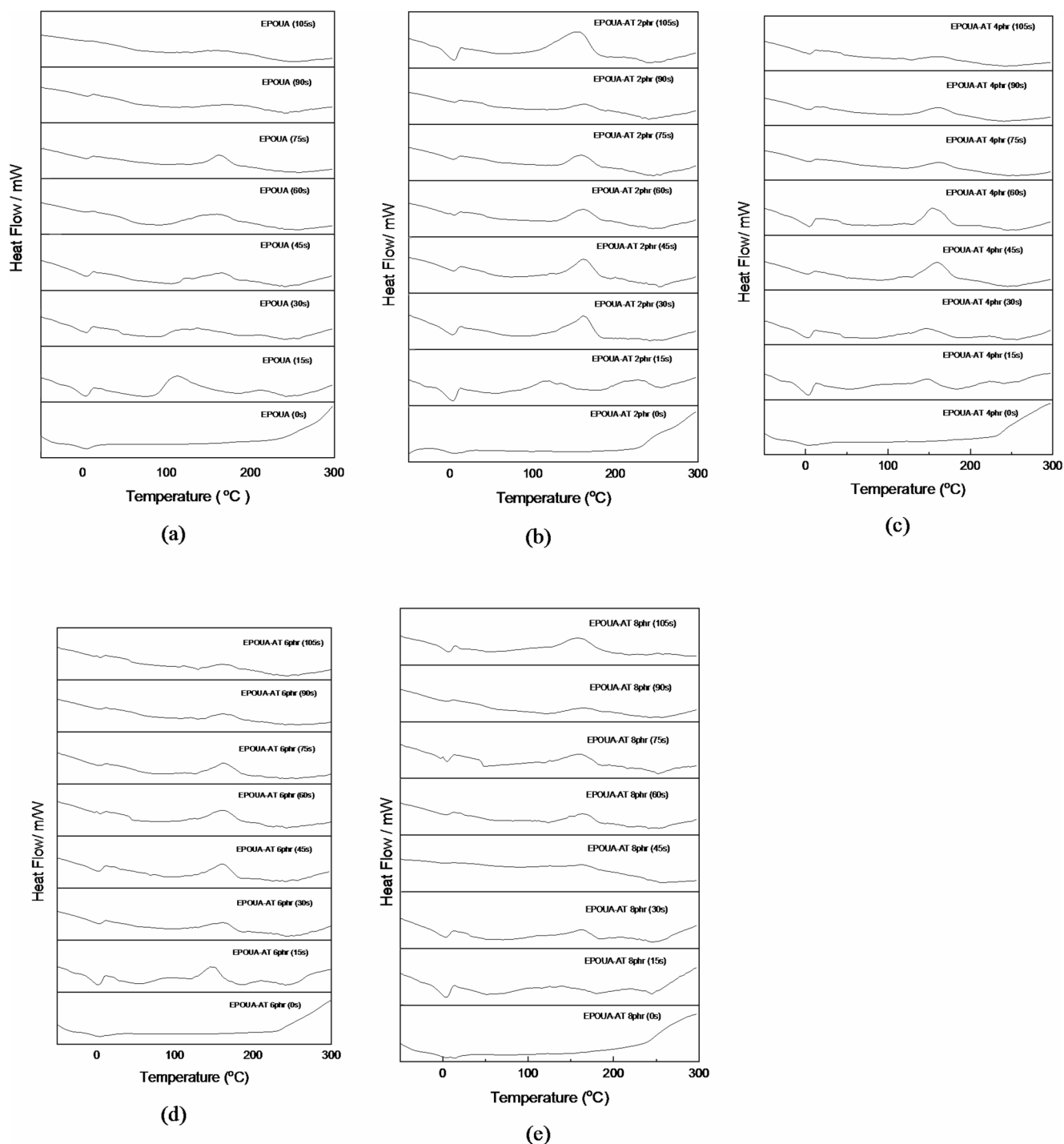


Fig. 3 DSC Analysis of EPOUA at Different Acrylation-Thiol (AT) addition and UV Exposure Time: (a) 0phr AT, (b) 2phr AT, (c) 4phr AT, (d) 6phr AT, and (e) 8phr AT

to ASTM D3363, the standard hardness for general paints typically falls between B and 3 H, depending on the formulation and intended application (ASTM International [3]). Therefore, the EPOUA-AT coatings, even at higher AT concentrations, exhibited sufficient hardness to meet industry standards for coatings used in protective applications.

Among all tested AT concentrations, the optimal balance between hardness and flexibility was observed at 2 to 4 phr AT, where the coatings retained adequate hardness without excessive brittleness.

Table 2 DSC results of EPOUA at different Acrylation-Thiol (AT) addition and UV exposure time

EPOUA-AT 0 phr					
Time of curing (s)	T _g (°C)	T _{crystallization} (°C)	ΔH crystallization (°C)	T _{onset curing} (°C)	ΔH curing (up to 300 °C)
0	4.72			212.01	1426.69
15	5.35	81.20	44.97	240.40	24.87
30	5.12	96.03	49.85	247.91	30.03
45	6.17	108.03	44.58	254.74	16.73
60	5.73	109.20	40.52	256.40	16.59
75	5.20	128.80	42.28	257.96	14.40
90	5.77	137.58	34.75	252.40	26.93
105	6.01	140.02	65.66	252.40	17.76
EPOUA-AT 2 phr					
Time of curing (s)	T _g (°C)	T _{crystallization} (°C)	ΔH crystallization (°C)	T _{onset curing} (°C)	ΔH curing (up to 300 °C)
0	6.30			225.47	1066.39
15	5.04	85.98	6.30	252.69	23.16
30	5.52	98.59	5.04	257.08	30.56
45	5.54	108.71	5.52	257.86	12.36
60	5.92	124.71	5.54	258.74	16.53
75	5.14	132.71	5.92	255.13	14.88
90	5.16	138.00	5.14	255.52	26.40
105	5.38	139.14	5.16	255.52	17.67
EPOUA-AT 4 phr					
Time of curing (s)	T _g (°C)	T _{crystallization} (°C)	ΔH crystallization (°C)	T _{onset curing} (°C)	ΔH curing (up to 300 °C)
0	5.03			233.18	1057.36
15	5.66	87.64	5.03	240.40	23.51
30	5.58	89.59	5.66	238.74	15.71
45	5.57	126.37	5.58	257.57	12.72
60	5.60	130.37	5.57	260.40	14.20
75	5.99	135.14	5.60	259.13	14.23
90	6.38	136.80	5.99	263.13	18.02
105	6.38	138.75	6.38	266.74	12.29
EPOUA-AT 6 phr					
Time of curing (s)	T _g (°C)	T _{crystallization} (°C)	ΔH crystallization (°C)	T _{onset curing} (°C)	ΔH curing (up to 300 °C)
0	5.21			231.91	856.01
15	5.60	105.98	5.21	258.35	20.50
30	5.21	129.97	5.60	263.52	12.69
45	4.82	134.75	5.21	262.35	11.62
60	5.60	133.97	4.82	268.78	13.76
75	5.21	137.58	5.60	265.57	13.98
90	5.21	143.14	5.21	266.35	16.44
105	5.99	147.14	5.21	269.57	13.85
EPOUA-AT 8 phr					
Time of curing (s)	T _g (°C)	T _{crystallization} (°C)	ΔH crystallization (°C)	T _{onset curing} (°C)	ΔH curing (up to 300 °C)
0	5.21			242.35	679.11
15	5.60	115.15	5.21	259.40	20.84
30	5.21	124.02	5.60	264.96	12.23
45	4.82	127.15	5.21	264.40	11.81

Table 2 (continued)

EPOUA-AT 8 phr					
Time of curing (s)	T _g (°C)	T _{crystallization} (°C)	ΔH crystallization (°C)	T _{onset curing} (°C)	ΔH curing (up to 300 °C)
60	5.60	132.02	4.82	272.78	13.29
75	5.21	137.97	5.60	271.13	13.53
90	5.21	141.97	5.21	274.74	16.22
105	5.99	140.41	5.21	275.52	12.41

Scanning Electron Microscopy (SEM)

Table 7 shows the SEM images of EPOUA at different concentration of AT modifications. Based on the table, the EPOUA image shows a clear and irregular structure at the cross-section when magnified up to 1000×. As AT is added to the formulation, the cross-section of EPOUA-AT becomes more organized, with a root-like pattern emerging as the AT concentration increases. This pattern becomes more pronounced at the highest AT addition (8 phr). Additionally, a distinct ‘Y’ pattern is observed at 8000× magnification in samples containing AT concentrations ranging from 2 phr to 8 phr. A possible explanation for this phenomenon is that AT, acting as a crosslinker, promotes the rearrangement of polymer structures into a more organized network, enhancing the polymer chain alignment (Kasetaitė et al. [13]).

Adhesion Test

Tables 8, 9 and 10 presents the adhesion test analysis of EPOUA and EPOUA-AT modified coatings. Overall, the results indicate that adhesion strength was higher on steel and plywood compared to glass. The percent area removed by tape on steel and plywood was 0%, meaning the edges of the cuts remained completely smooth, and none of the squares of the lattice detached, classifying them under the 5B category, which denotes excellent adhesion. The superior adhesion on steel and plywood can be attributed to their higher surface roughness, which promotes better mechanical interlocking between the coating and the substrate (Yang et al. [27]). In contrast, glass, being a smoother surface, provides less anchoring potential for coatings, leading to weaker adhesion. On the glass substrate, results showed that EPOUA and EPOUA-AT at 2 phr AT exhibited 0% detachment, maintaining smooth-cut edges and classifying under the 5B category. However, at 4, 6, and 8 phr AT, the coatings on glass exhibited severe flaking and detachment, leading to a 0B classification. This suggests that higher AT concentrations may increase film brittleness or reduce adhesion strength due to excessive crosslinking, limiting the coating’s ability to conform to the glass surface.

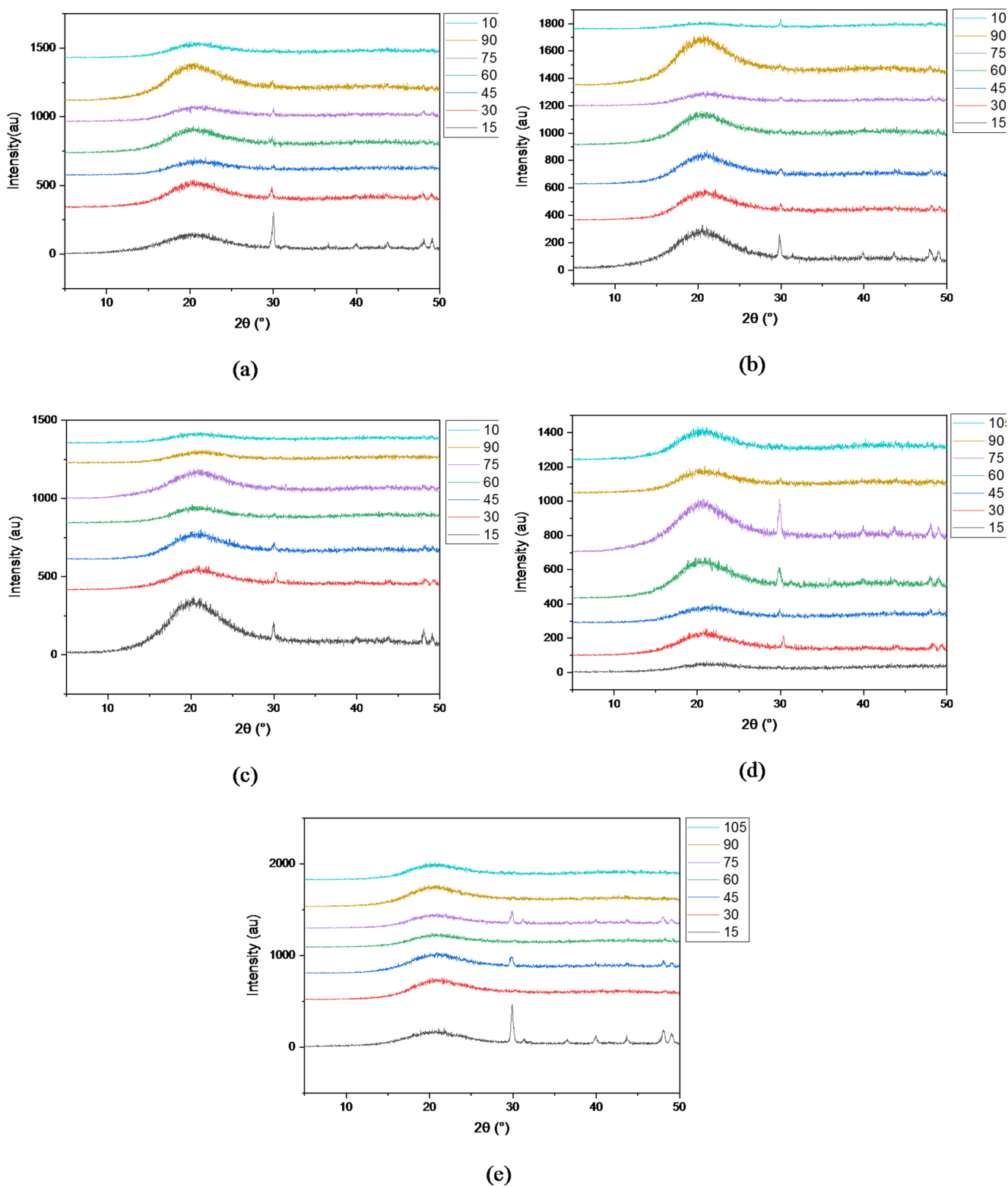
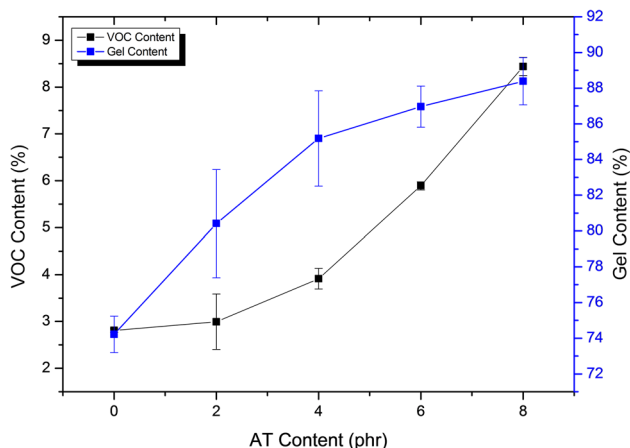


Fig. 4 XRD Analysis of EPOUA at Different Acrylation-Thiol (AT) addition and UV Exposure Time: (a) 0phr AT, (b) 2phr AT, (c) 4phr AT, (d) 6phr AT, and (e) 8phr AT

Table 3 The VOCs content of the cured samples

Acrylation-thiol (AT) Content (phr)	Gel Content (%)	VOCs Content (%)
0	74.22 ± 1.47	2.81 ± 0.08
2	80.41 ± 0.24	2.99 ± 0.05
4	85.18 ± 0.97	3.91 ± 0.03
6	86.96 ± 0.39	5.89 ± 0.26
8	88.39 ± 1.41	8.44 ± 0.07

**Fig. 5** Relationship of VOC and Gel Content at different AT concentration in EPOUA

Conclusion

This study demonstrated that the incorporation of acrylation thiol (AT) significantly improved the curing efficiency, crosslinking density, and physicochemical properties of epoxidized palm oil polyurethane acrylate (EPOUA) coatings. FTIR analysis confirmed the successful thiol-ene reaction, with the disappearance of the S-H peak and the formation of C-S bonds, indicating enhanced polymerization. Curing analysis showed that AT accelerated the curing process, reducing the curing time by 15 and 30 s at 2 and 4 phr AT, respectively. The improved curing performance also supported by the better crosslinking density as proven by the increased gel content by 8% at 2 phr and 15% at 4 phr, while maintaining the low VOC emissions which optimal at 4phr AT addition with 3.9% releases. Addition of AT to form double acrylation-thiol modification approach also improve the hardness properties of EPOUA coating. Addition of 2 and 4 phr AT proven improved the coating's hardness by threefold and fourfold, respectively. The SEM images of more structured and organized polymer network supports the better crosslinking and hardness properties of the EPOUA-AT coatings. Finally, the addition of AT also proven not disturb the high adhesion properties of EPOUA on plywood and steel substrate. Overall, 4 phr AT was identified as the optimal formulation, achieving faster curing

(60 s), high crosslinking (85% gel content), controlled VOC release (3.9%), improved hardness (4 H on glass, 3 H on plywood and steel), and strong adhesion (5B on steel, plywood, and aluminum). These findings demonstrate that AT-modified EPOUA coatings provide an effective, sustainable, and high-performance alternative for industrial applications, offering enhanced curing efficiency, durability, and mechanical properties while maintaining environmental compliance.

Table 4 Pencil hardness grade for EPOUA at different AT additions (Glass)

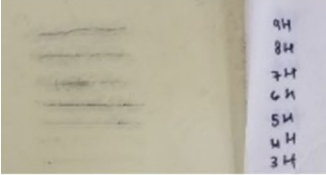
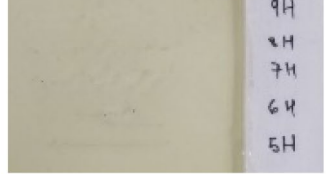
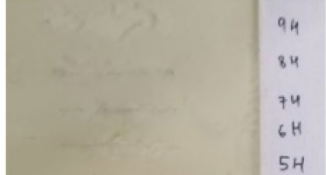
Acrylation Thiol (AT) Content	Result	Index
0 phr		H
2 phr		3H
4 phr		4H
6 phr		5H
8 phr		5H

Table 5 Pencil hardness grade for EPOUA at different AT additions (Plywood)

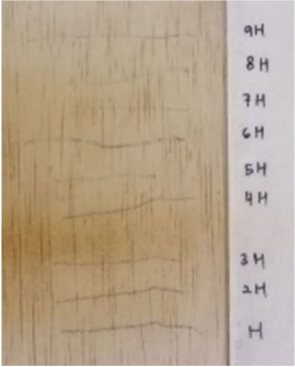
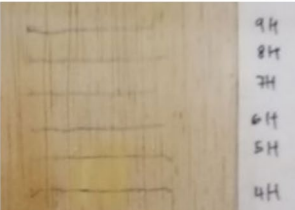
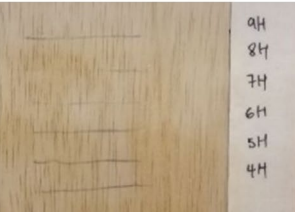
Acrylation Thiol (AT) Content	Result	Index
0 phr		H
2 phr		2H
4 phr		3H
6 phr		4H
8 phr		4H

Table 6 Pencil hardness grade for EPOUA at different AT additions (Steel)

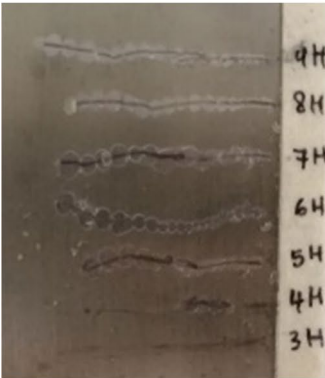
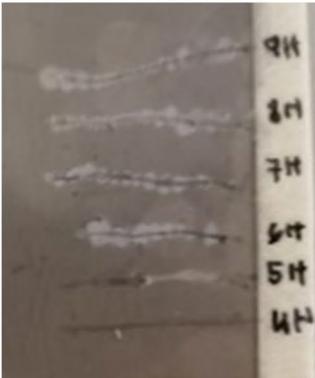
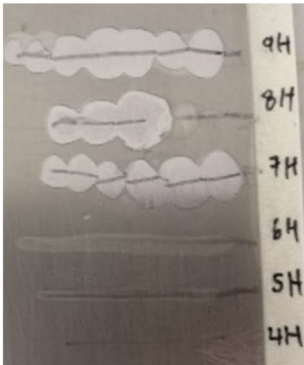
Acrylation Thiol (AT) Content	Result	Index
0 phr		8H
2 phr		6H
4 phr		3H
6 phr		4H
8 phr		4H

Table 7 SEM images of EPOUA fil at different AT Concentrations

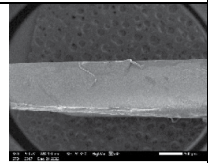
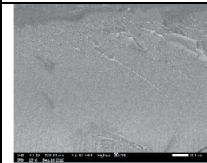
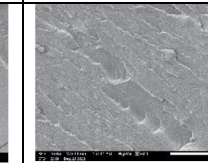
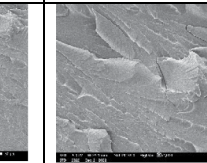
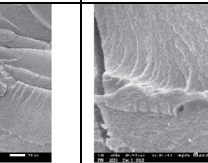
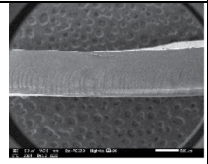
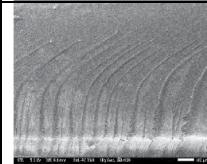
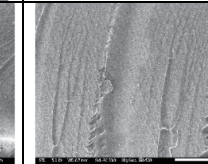
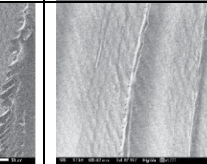
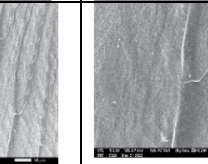
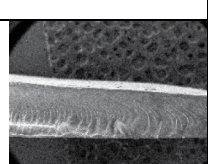
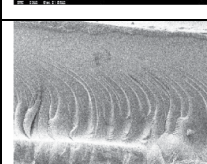
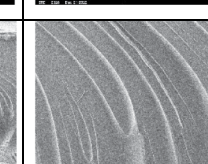
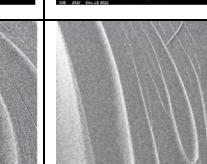
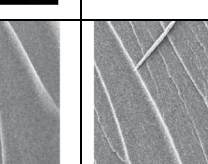
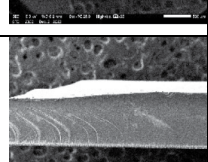
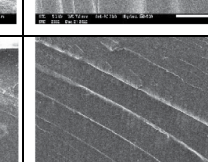
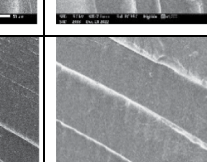
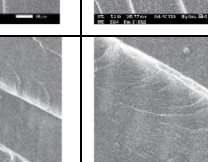
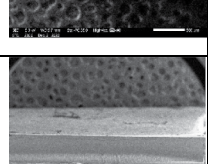
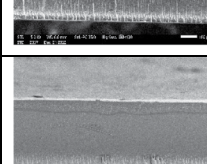
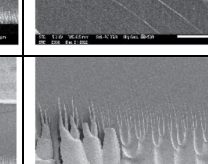
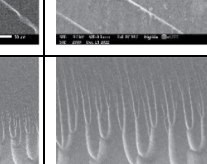
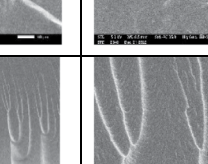
Sample	30x	100x	500x	1000x	8000x
EPOUA					
EPOUA-AT (2phr)					
EPOUA-AT (4phr)					
EPOUA-AT (6phr)					
EPOUA-AT (8phr)					

Table 8 Glass surface before and after adhesion test with grade

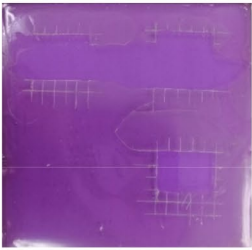
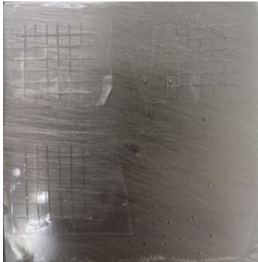
Acrylation Thiol (AT) Content	Before Test	After Test	Class
0 phr			5B
2 phr			5B
4 phr			0B
6 phr			0B
8 phr			0B

Table 9 Plywood surface before and after adhesion test with grade

Acrylation Thiol (AT) Content	Before Test	After Test	Class
0 phr			5B
2 phr			5B
4 phr			5B
6 phr			5B
8 phr			5B

Table 10 Plywood surface before and after adhesion test with grade

Acrylation Thiol (AT) Content	Before Test	After Test	Class
0 phr			5B
2 phr			5B
4 phr			5B
6 phr			5B
8 phr			5B

Acknowledgements This work was supported by the Ministry of Higher Education (MOHE) through the Fundamental Research Grant Scheme (FRGS) under grant no FRGS/1/2021/STG05/UMP/02/2 (RDU210105) and Fundamental Research Grant from Universiti Malaysia Pahang Al-Sultan Abdullah (RDU230309). The author would also like to thank PolyGreen (M) Sdn Bhd for providing the palm oil for this research.

Author Contributions Siti Noor Hidayah: Supervisor, Grant receiver, re-write the manuscript from the report submitted by the research assistants, Monitoring the overall characterization and method/approach conducted in this manuscript. Mohammad Ismail: Research assistant, provide basic result analysis of chemical characterization, conduct lab work. Muhammad Safwan: Research assistant, provide basic result analysis of the physical characterization, conduct lab work. Rasidi: Review the overall manuscript and provide suggestions in terms of chemical analysis. Rohani: Review the overall manuscript and provide suggestions in terms of physical analysis. Mohd Jumain: Review the overall manuscript and provide suggestions in terms of chemical analysis.

Funding Open access funding provided by The Ministry of Higher Education Malaysia and Universiti Malaysia Pahang Al-Sultan Abdullah

Data Availability No datasets were generated or analysed during the current study.

Declarations

Competing interest The authors declare that they have no known competing financial interests or personal relationships that could have appeared to influence the work reported in this paper.

Declaration of generative AI Author would like to declare that this manuscript is free from using AI tools.

Open Access This article is licensed under a Creative Commons Attribution-NonCommercial-NoDerivatives 4.0 International License, which permits any non-commercial use, sharing, distribution and reproduction in any medium or format, as long as you give appropriate credit to the original author(s) and the source, provide a link to the Creative Commons licence, and indicate if you modified the licensed material. You do not have permission under this licence to share adapted material derived from this article or parts of it. The images or other third party material in this article are included in the article's Creative Commons licence, unless indicated otherwise in a credit line to the material. If material is not included in the article's Creative Commons licence and your intended use is not permitted by statutory regulation or exceeds the permitted use, you will need to obtain permission directly from the copyright holder. To view a copy of this licence, visit <http://creativecommons.org/licenses/by-nc-nd/4.0/>.

References

- Abu Bakar NH, Salih N, Razali A (2020) Development of bio-based UV-curable coatings: utilization of palm oil derivatives. *J Coat Sci Technol* 12(3):214–229. <https://doi.org/10.1016/j.jcst.2020.03.005>
- Ali MF, Hassan MZ, Jafar Z (2022) Utilization of palm oil waste as a filler in sustainable concrete coatings. *Mater Today: Proc* 45:98–110. <https://doi.org/10.1016/j.matpr.2022.01.012>
- ASTM International (2011) *ASTM D3363-05: Standard test method for film hardness by pencil test*. ASTM International. Retrieved from <https://www.astm.org/d3363-05.html>
- Bowman CN, Kloxin CJ (2012) Toward an enhanced understanding and implementation of photopolymerization reactions. *AIChE Journal*, 58(5), 1284–1295. <https://doi.org/10.1002/aic.13765>
- Cheong YK, Tan WK, Lee CH (2016) Application of acrylated palm oil in UV-curable coatings. *Journal of Renewable Materials*, 4(2), 95–103. <https://doi.org/10.7569/JRM.2016.634106>
- Consumer Reports (2008) *Low-VOC paints: Safer for you and the environment*. Retrieved from <https://www.consumerreports.org>
- EPA (2008) *National volatile organic compound emission standards for consumer and commercial products*. U.S. Environmental Protection Agency. Retrieved from <https://www.epa.gov>
- Hashim H, Ahmad S, Hassan A (2021) Enhancement of flexibility in polyaniline-based conductive coatings using palm oil. *J Appl Polym Sci* 138(12):50123. <https://doi.org/10.1002/app.50123>
- He X, Xu X, Bo G, Yan Y (2020) Studies on the effects of different multiwalled carbon nanotube functionalization techniques on the properties of bio-based hybrid non-isocyanate polyurethane. *RSC Adv* 10(4). <https://doi.org/10.1039/c9ra08695a>
- Hoyle CE, Bowman CN (2010) Thiol–ene click chemistry: A powerful and versatile methodology for materials synthesis. *Angewandte Chemie International Edition*, 49(9), 1540–1573. <https://doi.org/10.1002/anie.200903924>
- Hu G, Christopher B, John AP, Annette FT (2010) Time-lapse thiol-acrylate polymerization using a pH clock reaction. *Journal of Polymer Science: Part A: Polymer Chemistry*, 48(13), 2955–2959. <https://doi.org/10.1002/pola.24088>
- Kadir MRA, Ahmad SH, Mahmood MH (2019) Utilization of palm oil as a green diluent in diamond-like carbon coatings. *J Mater Res Technol* 8(2):2224–2232. <https://doi.org/10.1016/j.jmr.2019.01.009>
- Kasetaite S, Flor SDL, Serra A, Ostrauskaite J (2018) Effect of selected thiols on Cross-Linking of acrylated epoxidized soybean oil and properties of resulting polymers. *Polymers* 10(4):439. <https://doi.org/10.3390/polym10040439>
- Kosheela T, Ramli A, Mahmud S (2015) Synthesis and characterization of acrylated epoxidized palm oil polyurethane. *Polym Test* 42:112–118. <https://doi.org/10.1016/j.polymertesting.2015.04.007>
- Ligon SC, Husár B, Wutzel H, Holman R, Liska R (2014) Strategies to reduce oxygen inhibition in photoinduced polymerization. *Chem Rev* 114(1):557–589. <https://doi.org/10.1021/cr3005197>
- Mohamad Isa MI, Mustapha SNH (2023) Enhanced hydrophobic performance of UV-curable palm oil polyurethane by uoroacrylate monomer. *Int J Polym Anal Charact* 28(5):1–19. <https://doi.org/10.1080/1023666X.2023.2244823>
- Mohamad Isa MI, Roslan R, Salim N, Mustapha R, Mustapha S. N. H. (2024) Synthesis and physicochemical properties of UV curable palm Oil-Based polyurethane reinforced with fluoroacrylate monomer. *J Polym Res* 31(197):2024. <https://doi.org/10.21203/rs.3.rs-3957274/v1>
- Mudri NH, Abdullah LC, Aung MM, Salleh MZ, Biak DRA, Rayung M (2020) Comparative study of aromatic and Cycloaliphatic isocyanate effects on physico-chemical properties of bio-based polyurethane acrylate coatings. *Polymers* 12(7). <https://doi.org/10.3390/polym12071494>
- Ooi TL, Salmiah A, Hazimah AH, Chong YJ (2006) An overview of R&D in palm oil-based polyols and polyurethanes in MPOB. *Palm Oil Developments*, 44, 1–7.
- Paraskar PM, Kulkarni RD (2021) Synthesis of isostearic acid/dimer fatty Acid-Based polyesteramide polyol for the development of green polyurethane coatings. *J Polym Environ* 29:54–70. <https://doi.org/10.1007/s10924-020-01849-x>

21. Paraskar P, Shukla S, Patil S (2020) The effect of chemical cross-linking on the thermal and mechanical properties of polyurethane systems. *J Polym Sci* 58(10):1125–1138. <https://doi.org/10.1002/pol.202058>
22. Rahman SHA, Ibrahim NA, Zainuddin N, Ariffin H (2021) Recent developments in vegetable oil-based ultraviolet (UV) curable coatings: A review. *Prog Org Coat* 151:106057. <https://doi.org/10.1016/j.porgcoat.2020.106057>
23. Salih A, Ahmad M, Ibrahim N, Dahlan K, Tajau R, Mahmood M, Yunus W (2015) Synthesis of radiation curable palm Oil-Based epoxy acrylate: NMR and FTIR spectroscopic investigations. *Molecules* 20(8):14191–14211. <https://doi.org/10.3390/molecules200814191>
24. Smith JD, Brown PR, Taylor LM (2021) Advances in UV-curing technology: A comprehensive review. *J Coat Technol Res* 18(5):1235–1250. <https://doi.org/10.1007/s11998-021-00478-9>
25. Tajau R, Ramli A, Hussin R (2014) UV-curable palm oil-based coatings: A study on urethane acrylate and acrylate epoxy formulations. *Surf Coat Int Part B: Coat Trans* 97(2):97–106. <https://doi.org/10.1007/s11998-014-0062-5>
26. Teo PS, Hassan A, Gan SN (2018) UV-curable palm oil-based resins: synthesis, characterization, and performance evaluation. *Prog Org Coat* 123:200–208. <https://doi.org/10.1016/j.porgcoat.2018.07.019>
27. Yang H, Du G, Li Z, Ran X, Zhou X, Li T, Gao W, Li J, Lei H, Yang L (2021) Superstrong adhesive of Isocyanate-Free polyurea with a branched structure. *ACS Appl Polym Mater* 3(3). <https://doi.org/10.1021/acsapm.1c00056>

Publisher's Note Springer Nature remains neutral with regard to jurisdictional claims in published maps and institutional affiliations.